Talanta 77 (2009) 943–947

Contents lists available at ScienceDirect

Talanta

journal homepage: www.elsevier.com/locate/talanta

Mesoporous silica hollow sphere (MSHS) for the bioelectrochemistry of horseradish peroxidase

Zhaoxia Cao[a,b], Jian Zhang[a,b], Julan Zeng[a,c], Lixian Sun[a,*], Fen Xu[a,*], Zhong Cao[c], Ling Zhang[c], Daowu Yang[c]

[a] Dalian Institute of Chemical Physics, Chinese Academy of Sciences, Materials & Thermochemistry Laboratory, 457 Zhongshan Road, Dalian 116023, Liaoning Province, China
[b] Graduate School of the Chinese Academy of Sciences, Beijing 100049, China
[c] School of Chemistry and Environmental Engineering, Changsha University of Science and Technology, Changsha 410076, China

ARTICLE INFO

Article history:
Received 3 March 2008
Received in revised form 10 June 2008
Accepted 15 June 2008
Available online 5 July 2008

Keywords:
Hollow mesoporous silica spheres
Horseradish peroxidase
Biosensor
Direct electron transfer

ABSTRACT

In this work, novel mesoporous silica hollow spheres (MSHS) were chosen as an immobilization matrix, to construct a mediator-free third-generation HRP biosensor. UV–vis spectroscopy revealed that horseradish peroxidase (HRP) entrapped in MSHS could retain its native structure. FTIR spectroscopy and nitrogen adsorption–desorption isotherms indicated that HRP are intercalated into the mesopores. The direct electron transfer of HRP entrapped in MSHS was observed. A pair of stable and well-defined redox peaks of HRP with a formal potential of about −0.150 V (vs. Ag/AgCl) in 0.1 M pH 7.0 phosphate-buffered solution (PBS) were obtained. The biosensor exhibited a fast amperometric response to H_2O_2 with a linear range of 3.9×10^{-6} to 1.4×10^{-4} M ($R = 0.997$, $N = 20$). The detection limit was 1.2×10^{-6} M based S/N = 3.

1. Introduction

Electrochemical sensors, such as third-generation amperometric biosensors, which are based on the direct electron transfer between the enzyme and the electrode, have attracted considerable attentions in recent years [1–3]. Direct electrochemical detection of hydrogen peroxide is of practical importance in chemical, biological, clinical, and many other fields. However, proteins exhibit a rather slow rate of heterogeneous electron transfer at conventional electrodes due to inaccessibility of the electroactive centers as well as its absorptive denaturation and unfavourable orientation of proteins on the electrode surface [4,5]. Therefore, the immobilization of enzyme is essential to the performance of biosensors.

In order to achieve direct electron transfer between HRP and electrode, surfactant [6], polymer [7,8], and nanomaterials like the inorganic oxide such as antimony oxide bromide (AOB) [9], TiO_2 [10], ZrO_2 [11,12], $CaCO_3$ [13] and composite materials [14–16] have been used as the immobilization matrices. Among these materials, mesoporous silicas (MSs), have several advantages [17–19]: MS possess large surface areas, highly ordered pore structures, very narrow pore size distributions, and variable pore diameters, and hence are good candidates as host materials for biomolecules [20,21].

Previous studies show that either mesostructure or morphology has a significant influence on the adsorption behavior of proteins and the performance of biosensor in addition to their framework composition and surface properties [22–26]. Liu et al. synthesized mesoporous silica of various morphologies and structures and investigated the lysozyme adsorption behaviors [27]. The highest lysozyme adsorption capacity of 536 mg g^{-1} was obtained on the mesoporous silica with cellular foam structure. Mesoporous hollow spheres with a rough surface exhibit the fastest adsorption rate and can adsorb more than 97% of lysozymes from the solution within 5 min.

Dai et al. reported that hexagonal mesoporous silicas (HMSs) can promote direct electrochemistry of many proteins such as myoglobin, hemoglobin and horseradish peroxide [28–30]. Taking account of the novel properties of silica hollow spheres (MSHS), it might serve as a promising host material for the redox protein to construct electrochemical biosensor. However, to our best knowledge, direct and unmediated voltammetry of HRP or any other redox enzyme incorporated in mesoporous silica hollow spheres has not been reported until now. In this paper, HRP was used as a simple model to study the feasibility of using this material in bioelectroanalysis. With isoelectric point (p*I*) at 8.8, HRP was positively charged at pH 7.0, and thus could easily assemble on this novel material which is negatively charged. As an enzyme immobilization

* Corresponding authors. Fax: +86 411 84379213.
E-mail addresses: lxsun@dicp.ac.cn, sunlixian168c@yahoo.com (L. Sun), fenxu@dicp.ac.cn (F. Xu).

0039-9140/$ – see front matter © 2008 Published by Elsevier B.V.
doi:10.1016/j.talanta.2008.06.043

matrix, MSHS can incorporate the enzyme through physical or chemical actions without the need for any complicated and time-consuming covalent attachment process. Combined with Nafion (a perfluorosulfonate linear polymer with excellent film-forming ability and stability), MSHS/entrapped with HRP was easily designed to construct a stable biosensor. The enzyme film could efficiently retain the bioactivity of the entrapped protein. Meanwhile, dramatically facilitated direct electron transfer of HRP and excellent bioelectrocatalytic activity towards H_2O_2 were obtained.

2. Experimental

2.1. Materials

HRP (EC 1.11 1.7, >250 U mg^{-1}) was from Sigma and used without further purification. Hydrogen peroxide (H_2O_2, 30%, w/w) was from Beijing Chemical Engineering Plant, its dilute solution was freshly prepared daily. Phosphate buffer solutions (PBS, 0.1 M) with different pH values were prepared by mixing the standard stock solutions of Na_2HPO_4 and NaH_2PO_4 and adjusting the pH with 1.0 M H_3PO_3 or NaOH. Other reagents were of analytical reagent grade and used as received. The method of synthesis of Mesoporous silica hollow sphere was described else where [27].

2.2. Measurements and apparatus

UV–visible (UV–vis) absorption spectroscopy was carried out by using a GBC-cintra 20 spectrophotometer. FTIR Spectra were obtained on a Bruker Equinox 55 Fourier transform infrared spectrometer (FTIR).

In adsorption experiments, 40 mg of mesoporous silica was dispersed in a solution of HRP (5 mg/mL, pH 7.0). The resulting mixture was continuously shaken in a shaking bath at room temperature for 24 h to reach adsorption equilibrium, then centrifuged at 10,000 rpm for 10 min. The supernatant was analyzed by UV absorbance at 403 nm. Adsorbed amounts were measured by the difference in the concentration of the enzyme before and after adsorption.

N_2 adsorption–desorption measurements were conducted on a micromeritrics ASAP 2000 apparatus at 77 K using nitrogen as the adsorption gas. MSHS (150 mg) was dispersed in a solution of HRP (5 mg/mL, pH 7.0) and shaken for 3 h for enzyme absorption. The bioconjugates, denoted as MSHS–HRP, were then centrifuged and washed with distilled water three times, and dried prior to N_2 adsorption–desorption measurements.

Electrochemical measurements were performed on an IM6e electrochemical workstation (Zahner-Elektrik, Kronach, Germany) with conventional three-electrode cell. The as-prepared enzyme electrode, a platinum electrode and an Ag/AgCl (saturated with NaCl) were used as the working electrode, counter electrode and reference electrode, respectively. All experimental solutions were deoxygenated by bubbling high-purity nitrogen for at least 20 min and maintained under nitrogen atmosphere during measurement. Experiments were carried out at room temperature ($18 \pm 2\,^{\circ}C$).

2.3. Preparation of enzyme electrodes

Prior to use, the glassy carbon electrode (GC, 3 mm in diameter) was polished to a mirror-like surface with 1.0, 0.3, and 0.05 μm alumina slurry followed by rinsing thoroughly with doubly distilled water. The electrodes were successively sonicated in 1:1 nitric acid, acetone and doubly distilled water in an ultrasonic bath, and then allowed to dry at room temperature.

The enzyme electrode was prepared by a simple casting method. Typically, 5 μL of a homogenous solution (pH 7.0) containing 2.5 mg mL^{-1} MSHS (pore size 11 nm), 2.5 mg mL^{-1} HRP and 1/5 (v_{nafion}/v_{total}) Nafion was dropped on the surface of pretreated GC electrode to prepare the HRP/MSHS/GC electrode. A breaker was covered over the electrode so that water can evaporate slowly in air and a uniform film electrode can be formed, the dried enzyme electrode was stored at 4 °C in refrigerator while not in use.

Table 1
Physicochemical properties of mesoporous silica and the amounts adsorbed of HRP.

Mesoporous silica	Pore diameter (Å)	BET surface area ($m^2\,g^{-1}$)	Total pore volume ($cm^3\,g^{-1}$)	Adsorbed amounts ($mg\,g^{-1}$)
MSHS-110	110	320	0.94	246
MSHS-90	90	758	1.00	216
MSHS-82	82	690	0.94	145

3. Results and discussion

3.1. Enzyme adsorption

The as-prepared samples have hollow spherical morphology with different pore sizes ranging from 8.2 to 11.0 nm, see in Ref. [27]. HRP molecules possess an oval-shaped structure with a molecular size of 4.3 nm × 3.7 nm × 6.4 nm which is smaller than the pore diameter of the hollow spherical samples. At pH 7.0, the HRP (p*I*, 8.8) should be positively charged, and the silica surface is negatively charged [31]. Thus the adsorption properties of the mesoporous material under the present conditions can be related to the mesostructure of the materials. The results of adsorption capacity of MSHS were summarized in Table 1.

The mesoporous hollow sphere materials showed the adsorption of large amounts of HRP, 141–246 mg g^{-1}. And MSHS with the largest pore diameter (11.0 nm) exhibited the highest HRP adsorption capacity. This is consistent with the findings of lysozyme adsorption behaviors [27].

Protein could be fixed in the pores of mesoporous materials by simply immersing the mesoporous material in the protein solution [32]. To clarify the effect of HRP on mesoporous materials, the N_2 adsorption isotherms after HRP loading were investigated (Fig. 1). For MSHS (pore size: 11 nm), the pore size decreased to 9.9 nm after HRP loading treatment and pore volume (0.64 $cm^3\,g^{-1}$) was 68.8% of that of MSHS (0.94 $cm^3\,g^{-1}$), indicating HRP intercalated into the

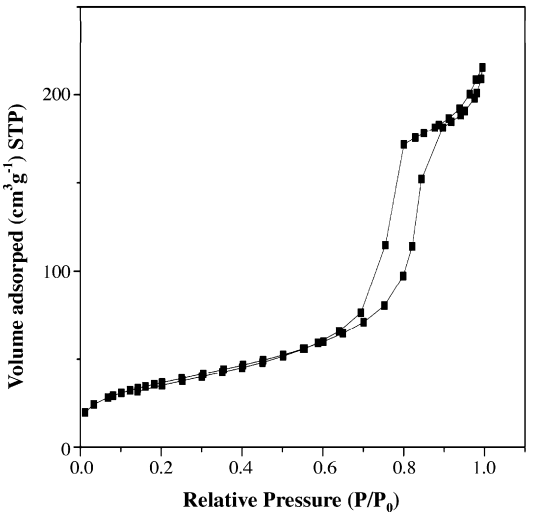

Fig. 1. N_2 adsorption–desorption isotherms after immobilizing of HRP on MSHS.

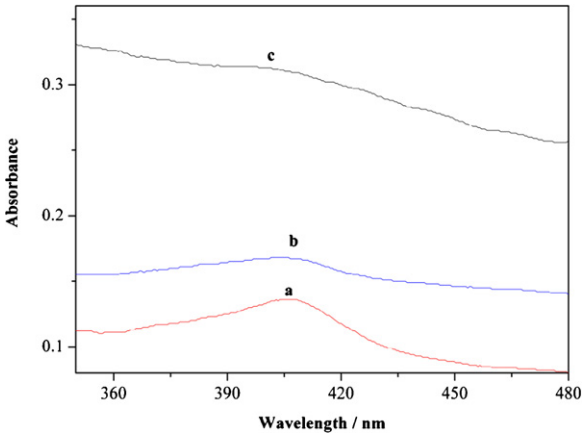

Fig. 2. UV–vis spectra of (a) HRP in solution, (b) dry MSHS/HRP and dry HRP/MSHS/Nafion composite films on quartz glass.

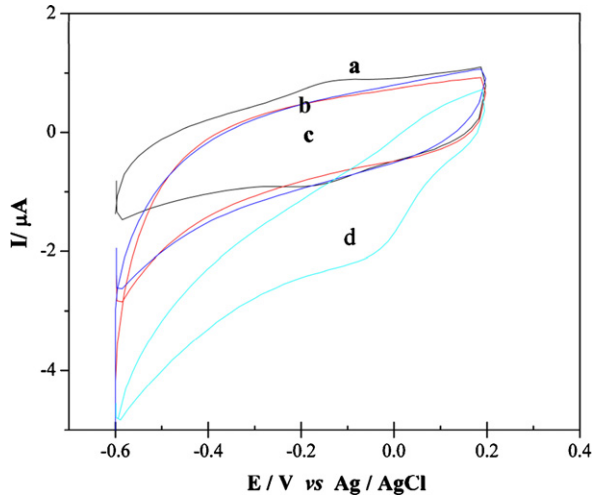

Fig. 4. CV of different modified electrodes in PBS (pH 7.0) at a scan rate of 100 mV s^{-1}: (a) HRP/MSHS/Nafion/GC, (b) MSHS/Nafion/GC, (c) bare GC and (d) HRP/Nafion/GC.

internal surface of MSHS [33]. Thus MSHS is a good matrix for HRP immobilization.

3.2. Spectroscopic characteristics of the MSHS/HRP

UV–vis spectroscopy is sensitive for the characteristic structure of proteins. The position of Soret absorption band of heme may provide information about possible denaturation of heme proteins. From Fig. 2, HRP entrapped in MSHS (curve b) or Nafion-MSHS (curve c) has a characteristic Soret absorption band at 403 nm, the same as that of native state of HRP in PBS (curve a), and retains its biological activity. This result suggests no significant denaturation occurs.

Fig. 3 shows the FTIR spectra of free HRP with that of HRP entrapped in the MSHS. For the pure MSHS (curve a) the absorption bands due to H_2O (1631 cm^{-1}), Si—O—Si (ν_{as}, 1092 cm^{-1}, ν_s, 804 cm^{-1}) and Si—OH (ν_s, 970 cm^{-1}) are observed, where ν_{as} = asymmetric stretching, ν_s = symmetric stretching [34]. This indicates that the as-formed MSHS contain a large amount of OH groups and H_2O on their surfaces [35]. Curve b is the FTIR spectrum of free HRP. The amide I band of HRP, which is caused by C=O stretching vibrations of peptide linkages, appears at 1654.9 cm^{-1}. The signal at 1535.3 cm^{-1} indicates the characteristic of amide II, which results from a combination of N—H in plane bending and C—N stretching vibrations of the peptide groups [36]. Curve c, the spectra of amide I and amide II bands (1656.8 and 1539.2 cm^{-1}) of HRP in MSHS are nearly the same as those obtained for native HRP. The similarities of the two spectra suggest that HRP retains the essential features of its native secondary structure in HRP–MSHS. The MSHS may provide a promising matrix for enzyme immobilization and biosensor fabrication because of its satisfactory biocompatibility. It should be pointed that upon adsorption of the HRP on MSHS, the bands at 1631 and 970 cm^{-1} shifted to 1656 and 985 cm^{-1}, respectively. The shift of water vibration adsorption band resulted from the interaction of NH_3^+ groups of HRP with Si groups in MSHS [37]. The shifts of framework vibration bands to higher frequency were due to the effect of the intercalated HRP on the pore size. This might result from the interaction between HRP and some specific sites on the pore internal surface of MSHS, consisting with the result of the N_2 adsorption isotherm.

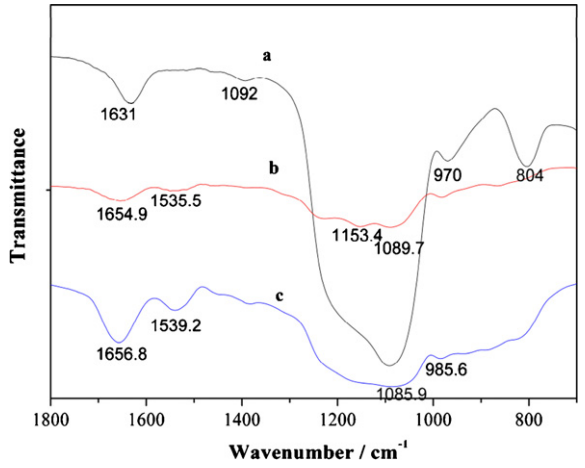

Fig. 3. FTIR spectra of (a) MSHS, (b) HRP and (c) MSHS/HRP.

3.3. Electrochemistry of HRP/MSHS/Nafion/GC electrode

Fig. 4 depicts the typical of HRP/MSHS/Nafion/GC (curve a), MSHS/Nafion/GC (curve b), bare GC (curve c) and HRP/Nafion/GC (curve d) electrode in 0.1 M phosphate buffer solution of pH 7.0 at 100 mV s^{-1}. As shown in CV (curve a), a pair of redox peaks was observed at the −0.217 and −0.085 V, which was related to the redox of the immobilized HRP. The low redox potential might imply special interactions between the molecular of HRP and MSHS, which could strongly affect the heme microenvironment. For HRP/Nafion/GC electrode, only a broad redox peak could be observed which shows that a direct electron transfer process could not take place. While the MSHS/Nafion/GC and bare GC displayed no redox peaks in the potential window, indicating electro-inactiveness. We also investigated the effect of pore size of MSHS on the properties of enzyme electrodes. The enzyme electrode modified with MSHS possessing largest pore size showed best performance (data not shown). So following electrochemistry measurements were done with MSHS (pore size: 11.0 nm).

Fig. 5 displays the direct electron transfer behavior of the immobilized HRP at various scan rates. With increasing scan rate, the redox peak currents of the adsorbed HRP increased, coupled with slightly enlarged peak-to-peak separation. The cathode peak currents showed linear response to scan rate from 50 to 1000 mV s^{-1} (inset of Fig. 5). All these result are in accordance with the surface-confined electrochemical behavior [38].

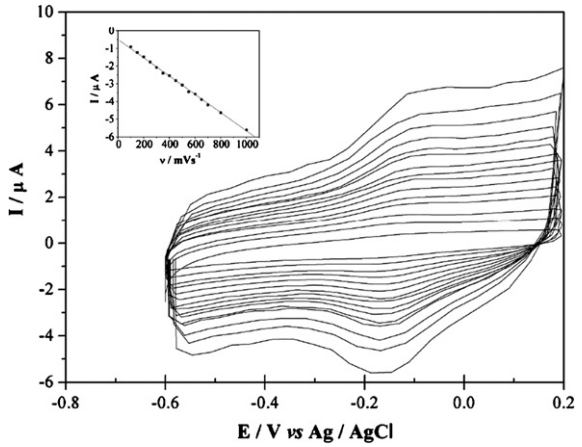

Fig. 5. CV of HRP/MSHS/GC electrode in PBS (pH 7.0) at 50, 100, 150, 200, 250, 300, 350, 400, 450, 500, 550, 600, 700, 800, 1000 mV s^{-1} (from inner to outer). Inset: plot of cathode peak current vs. scan rate.

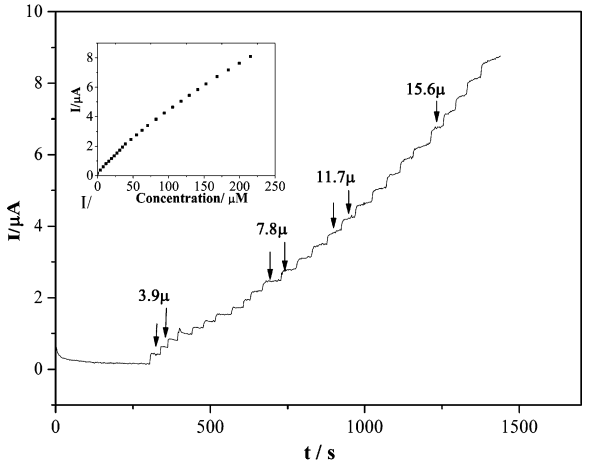

Fig. 7. Amperometric responses of HRP/MSHS/GC electrode upon successive additions of H_2O at −0.2 V in PBS (pH 7.0). Inset: plot of electrocatalytic current vs. H_2O_2 concentration.

3.4. Electrochemical response to hydrogen peroxide of HRP/MSHS/Nafion/GC electrode

The immobilized HRP undertakes a direct electron transfer reaction and exhibits an excellent electrocatalytic response to the reduction of H_2O_2 in PBS (Fig. 6). An obvious increase in the cathodic peak current was observed when H_2O_2 was added to a phosphate buffer indicating that a fast direct electron transfer reaction between the heme site of the immobilized HRP and the electrode surface was achieved [39,40]. These results illustrate that HRP in the MSHS can retain its bioelectrocatalytic activity.

As shown in Fig. 7, the amperometric response of the HRP/MSHS/Nafion/GC electrode to successive addition of different concentrations of H_2O_2 at the working potential of −0.2 V was also investigated. Upon addition of an aliquot of hydrogen peroxide to the buffer, the reduction current increased steeply to reach a stable value. The enzyme electrode achieved 95% of the steady-state current within 5 s. The calibration plot (inset of Fig. 7) shows a good linear response range to H_2O_2 in the wide range of 3.9×10^{-6} to 1.4×10^{-4} M ($R = 0.997$, $N = 20$), with detection limit of 1.2×10^{-6} M (S/N = 3) and sensitivity of 0.56 A m^{-1} cm^{-2}. Which is comparable to HRP immobilized in TiO_2 nanoparticle [41] film on PG electrode (linear response range: 7.5×10^{-6} to 1.23×10^{-4} M, detection limit: 2.5×10^{-6} M). The sensitivity is higher in comparison with that (0.184 A m^{-1} cm^{-2}) obtained by other immobilized HRP electrode reported previously [14]. The higher sensitivity may be related to novel architectures of MSHS that provided better mass transport and allowed more HRP loading. The apparent Michaelis–Menten constant (k_m) is calculated to be about 0.22 mM according to the Lineweaver–Burke equation, which was less than those of 1.38 mM for HRP immobilized in poly (ethylene glycol) [42], 2.3 mM for HRP immobilized on a colloid/cysteamine modified gold electrode [43] and 5.5 mM for HRP immobilized in polymer [40]. The small k_m shows a good affinity between the intercalated HRP in MSHS and H_2O_2.

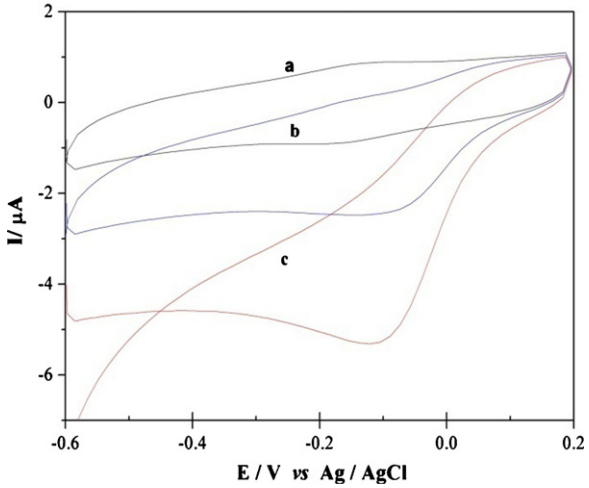

Fig. 6. Electrocatlysis of HRP/MSHS/Nafion/GC electrodes towards H_2O_2 in PBS (pH 7.0) at a scan rate of 100 mV s^{-1}. H_2O_2 concentrations: (a) 0 μM, (b) 7.8 μM and (c) 15.6 μM.

The stability of the enzyme electrode has been studied as well. Even the 50 continuous cyclic scans were carried out in the potential range from −0.6 to 0.2 V at a scan rate of 100 mV s^{-1}, no obvious change of the CV curve could be observed. When the electrode was stored in pH 7.0 PBS buffer solution at 4 °C for 20 days, the CV curve was still well retained, which suggested that the electrode had an excellent stability.

What we should point out is that MSHS is not suitable to construct a third-generation glucose biosensor according our experiments (see supplementary data). Although we could observe the direct electrochemistry of the glucose oxidase (GOD), the response was too poor to be used. The poor response may be due to a low GOD loading which resulted from the repulsion between GOD (p*I*, 4) and silica surface (both negatively charged) except a larger size than HRP molecular [31].

4. Conclusion

In this work, the direct electrochemical behavior of HRP immobilized in the silica hollow sphere and the feasibility of a reagentless mediator-free third-generation HRP biosensor has been investigated. The enzyme electrode has a fast response, wide linear detection range and low detection limit. The unique mesoporous silica hollow spheres could provide a desirable microenvironment for HRP to undergo facile electron transfer reaction. It also provides a good biosensing platform for redox-active proteins and enzymes, and may find wide potential applications in direct electrochemistry, biosensors, biocatalysis and biomedical devices.

Acknowledgments

The authors wish to express their gratitude and appreciation for Prof. Q.H. Yang, Dr. Liu Jian. This wok was supported by the National Natural Science Foundation of China (No. 50671098 and U0734005) and 863 projects (2007AA05Z115 and 2007AA05Z102).

Appendix A. Supplementary data

Supplementary data associated with this article can be found, in the online version, at doi:10.1016/j.talanta.2008.06.043.

References

[1] Y.H. Song, L. Wang, C.B. Ren, G.Y. Zhu, Z. Li, Sens. Actuators B 114 (2006) 1001–1006.
[2] Q. Xu, C. Mao, N.N. Liu, J.J. Zhu, J. Sheng, Biosens. Bioelectron. 22 (2006) 768–773.
[3] Y. Xu, W.J. Peng, X.J. Liu, G.X. Li, Biosens. Bioelectron. 20 (2004) 533–537.
[4] J.F. Rusling, Acc. Chem. Res. 31 (1998) 363–369.
[5] A. Heller, Acc. Chem. Res. 23 (1990) 128–134.
[6] K. Chattopadhyay, S. Mazumdar, Bioelectrochemistry 53 (2000) 17–24.
[7] Y.T. Kong, M. Boopathi, Y.B. Shim, Biosens. Bioelectron. 19 (2003) 227–232.
[8] S.Y. Xu, B. Peng, X.Z. Han, Biosens. Bioelectron. 22 (2007) 1807–1810.
[9] X.B. Lu, Z.H. Wen, J.H. Li, Biomaterials 27 (2006) 5740–5747.
[10] S.Q. Liu, A.C. Chen, Langmuir 21 (2005) 8409–8413.
[11] S.Z. Zong, Y. Cao, Y.M. Zhou, J.H. Xu, Langmuir 22 (2006) 8915–8919.
[12] Z.Q. Tong, R. Yuan, Y.Q. Chai, Y. Xie, S.H. Chen, J. Biotechnol. 128 (2007) 567–575.
[13] D. Shan, M.J. Zhu, H.G. Xue, S. Cosnier, Biosens. Bioelectron. 22 (2007) 1612–1617.
[14] W.Y. Cai, O. Xu, X.N. Zhao, J.J. Zhu, H.Y. Chen, Chem. Mater. 18 (2006) 279–284.
[15] L. Qian, X.R. Yang, Talanta 68 (2006) 721–727.
[16] Y. Liu, J.P. Lei, H.X. Ju, Talanta 74 (2008) 965–970.
[17] Y.J. Wang, F. Caruso, Chem. Mater. 17 (2005) 953–961.
[18] R. Ravindra, S. Zhao, H. Gies, R. Winter, J. Am. Chem. Soc. 126 (2004) 12224–12225.
[19] J. Fan, C. Yu, F. Gao, J. Lei, B. Tian, L. Wang, B. Tu, D. Zhao, Angew. Chem. Int. Ed. 42 (2003) 3146–3150.
[20] J. Lei, J. Fan, C. Yu, L. Zhang, S. Jiang, B. Tu, D. Zhao, Micropor. Mesopor. Mater. 73 (2004) 121–128.
[21] Y.Z. Xian, Y. Xian, L.H. Zhou, F.H. Wu, Y. Ling, L.T. Jin, Electrochem. Commun. 9 (2007) 142–148.
[22] J.M. Sun, H. Zhang, R. Tian, D. Ma, X. Bao, D.S. Su, H. Zou, Chem. Commun. 12 (2006) 1322–1324.
[23] S.Z. Qiao, H. Djojoputro, Q.H. Hu, G.Q. Lu, Prog. Solid State Chem. 34 (2006) 249–256.
[24] A. Vinu, V. Murugesan, M. Hartmann, J. Phys. Chem. B 108 (2004) 7323–7330.
[25] B. Li, H. Takahashi, Biotechnol. Lett. 22 (2000) 1953–1958.
[26] H. Takahashi, B. Li, T. Sasaki, C. Miyazaki, T. Kajino, S. Inagaki, Chem. Mater. 12 (2000) 3301–3305.
[27] J. Liu, C.M. Li, Q.H. Yang, J. Yang, C. Li, Langmuir 23 (2007) 7255–7262.
[28] Z.H. Dai, X.X. Xu, H.X. Ju, Anal. Biochem. 332 (2004) 23–28.
[29] Z.H. Dai, S.Q. Liu, H.X. Ju, H.Y. Chen, Biosens. Bioelectron. 19 (2004) 861–867.
[30] Z.H. Dai, H.X. Ju, H.Y. Chen, Electroanalysis 10 (2005) 862–868.
[31] H. Liu, P. Wright, J. Mater. Chem. 15 (2005) 3690–3700.
[32] J.F. Diaz, K.J. Balkus Jr., Mol. Catal. B: Enzym. 2 (1996) 115–126.
[33] H. Takahashi, B. Li, T. Sasaki, C. Miyazaki, T. Kajino, S. Inagaki, Micropor. Mesopor. Mater. 44 (2001) 755–762.
[34] M.W. Anderson, J. Klinowski, J. Chem. Soc. Faraday Trans. 1 (82) (1986) 1449–1469.
[35] A. Kioul, L. Mascia, J. Non-Cryst. Solids 175 (1994) 169–186.
[36] J.K. Kauppinen, D.J. Moffate, H.H. Mantsch, D.G. Cameron, Appl. Spectrosc. 35 (1981) 271–276.
[37] B. Liu, R. Hu, J. Deng, Anal. Chem. 69 (1997) 2343–2348.
[38] R.W. Murray, A.J. Bard (Eds.), Electroanaytical Chemistry, 13, Marcel Dekker, New York, 1984, p. 191.
[39] T. Ferri, A. Poscia, R. Santucci, Bioelectrochem. Bioenerg. 44 (1998) 177–181.
[40] T. Ferri, A. Poscia, R. Santucci, Bioelectrochem. Bioenerg. 45 (1998) 221–226.
[41] Y. Zhang, P.L. He, N.F. Hu, Electrochim. Acta 49 (2004) 1981–1988.
[42] Y. Xu, W. Peng, X. Liu, G. Li, Biosens. Bioelectron. 20 (2004) 533–561.
[43] Y. Xiao, H.X. Ju, H.Y. Chen, Anal. Biochem. 278 (2000) 22–28.